

## SUPPLEMENTARY DATA

### **Phase separation induced shell thickness variations in the Electrospun Hollow Bioglass 45S5 Fiber mats for Drug Delivery Applications**

**D. Durgalakshmi and S. Balakumar\***

\*National Centre for Nanoscience and Nanotechnology,  
University of Madras, Chennai-600 025, India.

[balasuga@yahoo.com](mailto:balasuga@yahoo.com)



**Figure S1.** Schematic representation of the fabrication of Bioglass fibers using the electrospinning technique. The Bioglass containing transparent solution has been diluted with ethanol or water and fed to the electrospinning setup. The high voltage power leads to the formation of fibers and it was collected using a drum collector.

**Table S2.** Optimization conditions of the Bioglass fibers and the inference obtained at different processing conditions.

<b>Dilution</b>	<b>Parameters</b>	<b>Average Fiber Size</b>	<b>Bead size</b>	<b>Inference</b>
Ethanol	0.3mL/h, 10 kV	985 nm		Thin fiber mat
Ethanol	0.3mL/h, 15 kV	920 nm		Thick fiber mat in good yield
Ethanol	0.2mL/h, 10 kV	600 nm – 1200 nm		Flat fibers
Ethanol	0.2mL/h, 15 kV	1020 nm		Flat fibers Found beads randomly
Water	0.3mL/h, 10 kV			No fiber formation
Water	0.3mL/h, 15 kV	170 nm – 180 nm	850 nm – 1000 nm	Beads with large gap in less yield
Water	0.2mL/h, 10 kV	190 nm – 200 nm	850 nm – 900 nm	Beads with large gap
Water	0.2mL/h, 15 kV	220 nm – 240 nm	820 nm – 950 nm	Beads with small gap

**Table S3.** Porosity analysis of Bioglass fibers.

<b>Sample code</b>	<b>Fiber Diameter (<math>\mu\text{m}</math>)</b>	<b>Specific surface Area (<math>\text{m}^2/\text{g}</math>)</b>	<b>Pore radius (<math>\mu\text{m}</math>)</b>	<b>Specific pore volume (<math>\text{cm}^3/\text{g}</math>)</b>
E	1.60	8.1305	0.1098	0.022
E+H	0.34	7.9984	0.1202	0.062
H	0.75	9.2916	0.1164	0.057

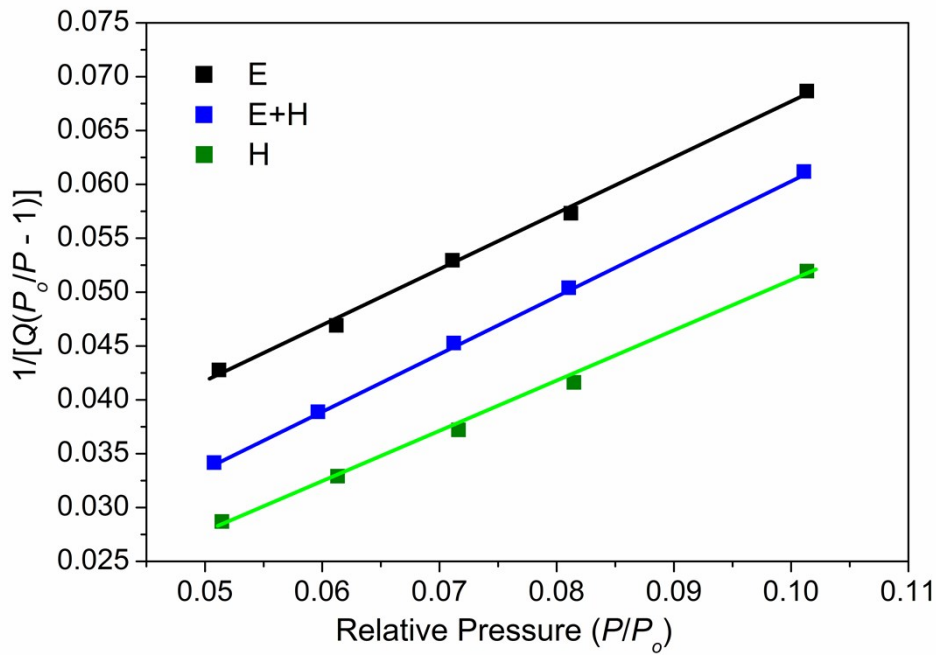


**Figure S4.** BET multipoint surface area analysis of the Bioglass fibers.

When the BET curve is plotted, the graph should be linear with a positive slope for obtaining the surface area. The linear plot given in Fig. 9 satisfies the consistency criterion and good fit.

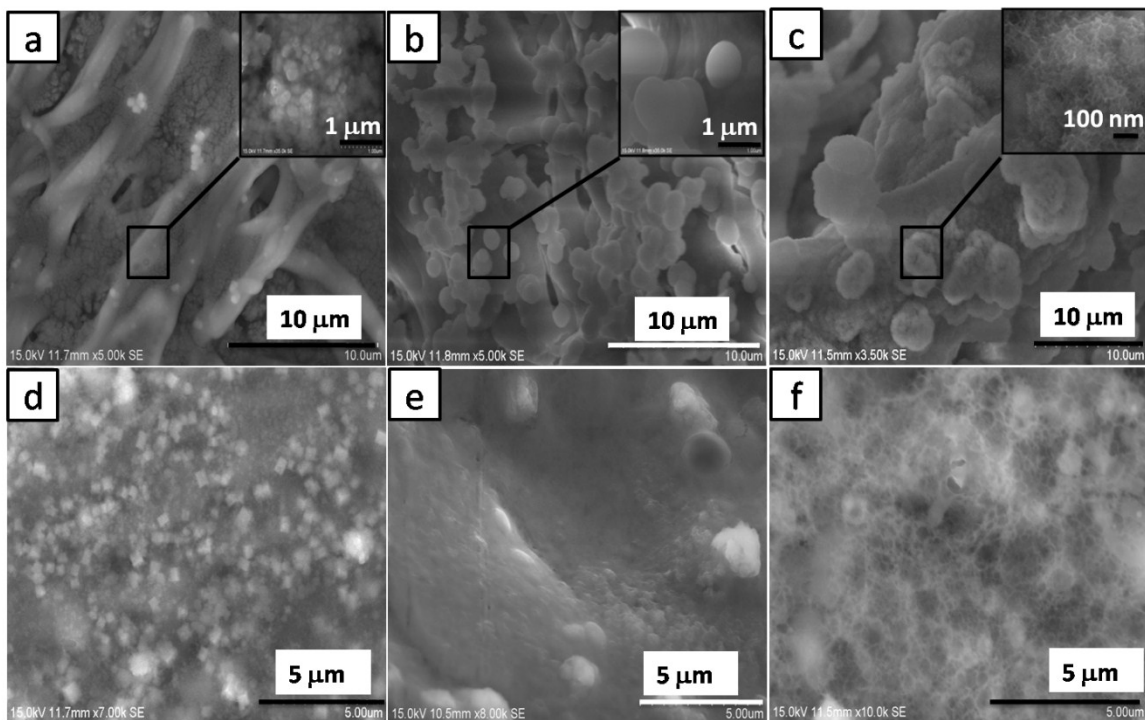


**Figure S5.** *In vitro* immersion studies of Bioglass fibers obtained under different dilution

conditions for 7<sup>th</sup> day ((a) ethanol, (b) E+H and (c) water) and 14<sup>th</sup> day ((d) ethanol, (e) E+H and (f) water).

When these were incubated for 7 day and 14 day, the fiber morphology was changed more significantly with the apatite formation, almost covering the entire surface. The 7<sup>th</sup> day immersion studies of the fibers (Fig. 11(a) –(c)) show that E+H prepared fibers were completely covered by apatite layer and surface of fibers were not visible (inset of Fig. 11(a) – (c)), where depends on the fiber diameter, the nucleation and apatite formation also varied. Water prepared samples show nucleation of a needle like apatite rods of size ~ 30nm on the surface; ethanol prepared samples show the next stage of needle formation to growth of the crystals; E+H diluted samples show spherical particles formed over the surface of apatite sheets. This confirms that lesser the diameter of the fibers higher is the apatite formation. Previously, Kim *et al.* also reported that Bioglass 70S nanofibers have higher biodegradation in SBF compared to microsized fibers [26]. This is due to the larger surface area of the nanosized fibers, which resulted in faster dissolution and super – saturation of the medium with respect to the apatite crystal nucleation. Further extension of these fibers to 14 days shows a complete covering of the surface by apatite bone minerals. The 14<sup>th</sup> day results also support the E+H prepared samples due to the smoother and evenly formed apatite layer.

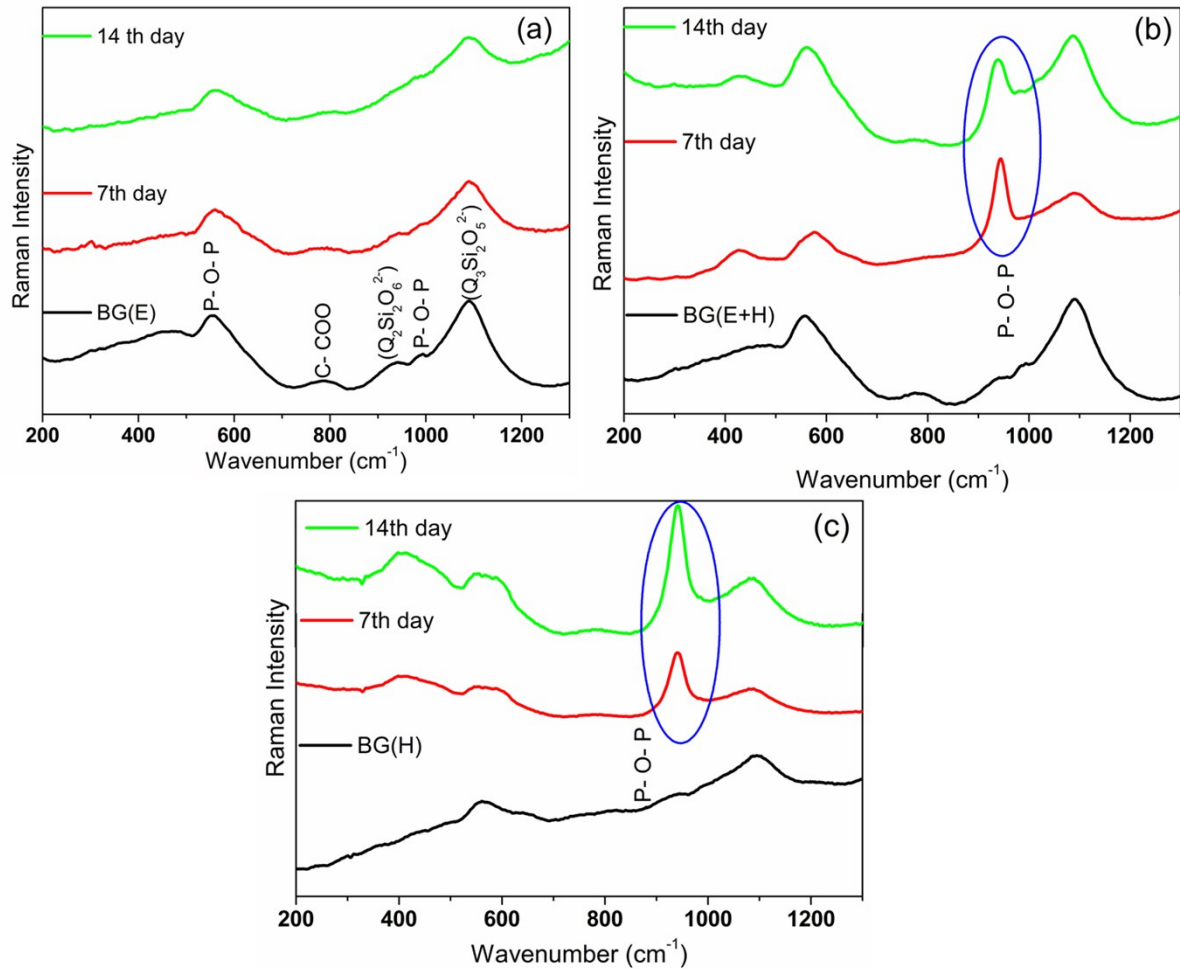


**Figure S6.** Micro-Raman studies of Bioglass fibers immersed in simulated body fluid solution after 7 day and 14 day.

The apatite formation onto the surface of Bioglass fibers were further analysed by micro – Raman spectroscopy as suggested by Nothinger *et al.* [27] and is shown in Fig. 12. As the incubation time increased, the bands related to the silica glass in the region of 700  $\text{cm}^{-1}$  to 1200  $\text{cm}^{-1}$  were attenuated. In general, the apatite formations on the surface of the samples after immersion were identified from the strong characteristic 960  $\text{cm}^{-1}$  phosphate peak corresponding to the P – O symmetrical vibration of the  $\text{PO}_4^{3-}$ . The peak at 960  $\text{cm}^{-1}$  increases with immersion time in SBF, which indicates that the amount of apatite formed on the surface increases with time. E+H prepared samples show a higher phosphate formation on the 7<sup>th</sup> day itself compared to the other fibers. For 14<sup>th</sup> day samples, in E+H prepared samples show a less intense phosphate peak and more intense silinol peak. This was due to the physio

– chemical reaction mechanism proposed by Hench *et al.* The dissolution of Ca, P, and Si from the fiber surface and subsequent precipitation of apatite crystals from the medium, with further immersion of fibers result in the leaching of Si, leading to an increase in the silinol peak after 14 days. However, the silinol peak will further degrade over the surface and it is a continuous process for the formation of bone mineral. For water prepared samples, the phosphate peak was increasing further, impling that the apatite formation was still progressing and it was not saturated. This result is in good agreement with the FESEM results discussed already.